Al-Rafidain J Med Sci. 2025;8(1):97-105.
DOI: https://doi.org/10.54133/ajms.v8i1.1687

AJMS

Online ISSN (2789-3219)

Research Article

Nanospanlastic *in situ* Gel for Nose to Brain Delivery of Nimodipine: *In vitro* Optimization and *in vivo* Pharmacokinetic Study

Hussein Kadhum Alkufi[1]*, Hanan Jalal Kassab[2]

[1]*Department of Pharmacognosy, College of Pharmacy, University of Thi-Qar, Thi-Qar 64001, Iraq;* [2]*Department of Pharmaceutics, College of Pharmacy, University of Baghdad, Baghdad, Iraq*

Received: 7 January 2025; Revised: 12 February 2025; Accepted: 14 February 2025

Abstract

Background: The FDA has approved the medication nimodipine (NMD) to treat vasospasm brought on by subarachnoid hemorrhage. The most popular way to administer NMD is intravenously, which can result in several adverse effects, including bradycardia, hypotension, arrhythmias, and inflammation at the administration site. ***Objective***: To evaluate the effectiveness of nose-to-brain (NTB) delivery of NMD as spanlastic nanovesicles (SNV) *in situ* gel into the brain and compare it with IV infusion. ***Methods***: The nanovesicle formulation by the ethanol injection method used Span 60 as a non-ionic surfactant and Tween 60 as an edge activator for enhanced permeability. The nanovesicle formulation is within the accepted range for nose-to-brain mixing with poloxamer 407 to *in situ* gel formulation by the cold method. ***Results***: The result was observed in the optimized formula with a particle size of 73.18 nm, a PDI of 0.1646, and higher drug entrapment within the vesicles. The *in situ* gel with the optimized formula shows gelation temperature with nasal fluid temperature. The *in vivo* pharmacokinetic behavior of NTB in the optimized formula in blood and brain was contrasted with commercial NMD. In contrast to intravenous administration of the NMD, the results indicate that NTB of NMD *in situ* gel was able to deliver the same amount of NMD to brain tissue with lower drug levels in blood. ***Conclusions***: The nose-to-brain approach for NMD-SNV may be able to deliver NMD systemically to the brain with less frequent dosing and fewer cardiac adverse effects.

Keywords: *In situ* gel, Nimodipine, Pharmacokinetic study, Probe pull test, Spanlastic nanovesicle.

هلام موضعي لتوصيل نيموديبين على شكل حويصلات نانوية مرنة من الأنف إلى المخ: تحسين في المختبر ودراسة الحركية الدوائية في الجسم الحي

الخلاصة

الخلفية: وافقت إدارة الغذاء والدواء الأمريكية على عقار نيموديبين لعلاج تشنج الأوعية الدموية الناتج عن نزيف تحت العنكبوتية. الطريقة الأكثر شيوعًا لإعطاء نيموديبين هي عن طريق الوريد، مما قد يؤدي إلى عدد من الآثار الجانبية، بما في ذلك بطء القلب وانخفاض ضغط الدم وعدم انتظام ضربات القلب والالتهاب في موقع الإعطاء. **الهدف**: تقييم فعالية توصيل نيموديبين من الأنف إلى المخ على شكل هلام موضعي للحويصلات النانوية السبانلاستيكية إلى المخ ومقارنته بالاعطاء الوريدي. **الطرائق**: استخدمت تركيبة الحويصلات النانوية بطريقة الحقن بالإيثانول مادة سبان 60 كمنشط سطحي غير أيوني وتوين 60 كمنشط حافة لتعزيز النفاذية. تركيبة الحويصلات النانوية ضمن النطاق المقبول لخلطها من الأنف إلى المخ مع بولوكسامير 407 لتركيبة هلام موضعي بطريقة باردة. **النتائج**: الصيغة المحسنة بحجم جسيم 73.18 نانومتر. يُظهر الجل الموجود في الموقع بالصيغة المحسنة درجة حرارة التجلط مع درجة حرارة السائل الأنفي، وتماسك جيد وقدرة على الالتصاق وقوة الهلام. تمت مقارنة السلوك الحركي الدوائي الحيوي لتوصيل عن طريق الانف في الصيغة المحسنة في الدم والدماغ مع نيمودبين التجاري. وعلى النقيض من الإعطاء الوريدي. **الأستنتاجات**: الاعطاء عن طريق الانف من الجل كان قادرًا على توصيل نفس كمية نيمودبين إلى أنسجة المخ بمستويات أقل من الدواء في الدم، وهو أمر مفيد للغاية لتقليل الآثار الجانبية القلبية الوعائية. مع معدل إخراج أبطأ ومستويات دم أقل. قد يكون نهج الأنف إلى الدماغ لنيموديبين الحويصلي قادرًا على توصيل نيموديبين بشكل منهجي إلى المخ بجرعات أقل وآثار جانبية قلبية أقل.

* ***Corresponding author***: Hussein K. Alkufi, Department of Pharmacognosy, College of Pharmacy, University of Thi-Qar, Thi-Qar 64001, Iraq; Email: husseinalkufi21@utq.edu.iq

Article citation: Alkufi HK, Kassab HJ. Nanospanlastic *in situ* Gel for Nose to Brain Delivery of Nimodipine: *In vitro* Optimization and *in vivo* Pharmacokinetic Study. *Al-Rafidain J Med Sci.* 2025;8(1):97-105. doi: https://doi.org/10.54133/ajms.v8i1.1687

INTRODUCTION

Heart disease is the main cause of death, with stroke coming in second. One to seven percent of strokes are caused by acute subarachnoid hemorrhage (SH), which is brought on by ruptured brain aneurysms after trauma [1]. For 25–50% of fatalities and 50% of permanent impairments, SH is to blame [2]. A 1,4-dihydropyridine L-type calcium ion channel antagonist with a high lipophilicity is nimodipine (NMD). Its main application is in the treatment of SH because it enhances cerebral blood flow and expands the cerebral arteries. NMD treats dementia and age-related neurodegenerative diseases because aging reduces intracellular calcium concentration. NMD's limited water solubility (3.86 µg/mL) and low bioavailability (5–13%) limit its therapeutic efficacy [3–5]. Additionally, because 98% of NMD is linked to plasma

proteins, comparatively little of it enters the brain when compared to its plasma levels in SH patients [6]. NMD is taken orally every four hours for 21 days in a row. 360 mg per day is the extremely high oral dosage needed to make up for its low bioavailability [7]. Most efforts to address the inadequate pharmacokinetic characteristics of NMD taken orally were successful in increasing its bioavailability. However, neither the frequency of the dose nor the drug's brain targeting efficiency (DTE%) was ascertained. The purpose of intravenous NMD delivery is to increase medication bioavailability. However, when administered parenterally at large levels, NMD causes several adverse effects, such as bradycardia, arrhythmias, and hypotension, which can ultimately result in death [8]. As a non-invasive method of avoiding the blood-brain barrier and delivering medications straight to the brain via the olfactory pathway, drug administration via the nose-to-brain route has attracted a lot of attention [9]. Encapsulating drugs in liposomes, nanoparticles, polymeric nano-carriers, and microspheres offers several advantages, including stability, solubilization of poorly soluble drugs, avoidance of precipitate upon dilution, and defense against destabilizing chemicals [10,11]. After transport from the nose to the brain, most nano-carrier systems show preferential absorption into the brain through the olfactory pathway. Improving the nose-to-brain pathway of NMD improved the intranasal NMD microemulsion and nanoparticles' ability to reach the brain [12]. Using lipid nanocapsules and NM-loaded lipo-pluronic micelles via the direct intranasal channel, our research team has already improved the transport of NMD to the brain [8,13]. Spanlastics are bendable nanocarriers that rely on surfactants. The majority of spanlastics are made of non-ionic surfactants and edge activators (EAs). By pushing through different biological layer pores without shattering, EAs destabilize the vesicular membranes of the nanocarriers, enhancing their permeability and flexibility across biological membranes. Flexible, safe, and biodegradable nanovesicles are known as nanospanlastics. Moreover, they exhibit higher chemical stability than conventional liposomes. Nanospanlastics is therefore a stable nanocarrier capable of containing NMD. Moreover, because spanlastics are flexible and can penetrate biological membranes' microscopic pores, they can increase NMD's penetration [14–19]. Drugs can be delivered via the nose-brain pathway (olfactory pathway) by intranasally given nano-carriers. Alternatively, it can enter the systemic circulation through the nasal epithelium and go to the brain across the blood-brain barrier (nose-blood-brain transport). It is still unclear how the olfactory and systemic pathways contribute to the drug's entry into brain regions following intranasal treatment of SNV [20–22]. The goal of this research is to create an NMD-loaded SNV *in situ* gel and examine if NTB can deliver NMD into the brain efficiently as a substitute for intravenous NMD with a comparable level of brain bioavailability.

METHODS

Materials

Nimodipine was purchased from Hyperchem in China. Ethanol was purchased from Honeywell International Inc., USA. Soluplus® was gifted from BASF, Germany. Span 60 and Tween 60 from Hyper Chem, China; Brij®-35 from Central Drug House, India. Dialysis bag 8-14 kDa Lab Pvt. Ltd., USA. Amicon ultrafilter with a MWCO of 3 kDa, purchased from Sigma-Aldrich, Merck. All other chemicals were of analytical grade.

Preparation of SNV formulations

The ethanol injection technique was used to manufacture spanlastic nanovesicles [23,24]. That is, five milliliters of pure ethanol were used to dissolve NMD and span 60. A magnetic stirrer was used to agitate the alcoholic solution at 1000 rpm and 60°C while it was gradually injected into a warm Tween 60 aqueous solution (10 ml) with Soluplus as a stabilizer. As indicated in Table 1, after an hour of stirring, the resultant dispersion was bath-sonicated for 30 minutes to remove any aggregates. The combinations were finally placed in the refrigerator for additional analysis.

Table 1: Formulations of NMD loaded SNV

Run	NMD (mg)	Span 60 (mg)	Tween 60 (mg)	Soluplus (mg)	Sonication time (min)	Total volume (ml)
SNV1	10	225	25	50	30	10
SNV2	10	175	75	50	30	10
SNV3	10	125	125	50	30	10
SNV4	10	225	25	50	0	10
SNV5	10	175	75	50	0	10
SNV6	10	125	125	50	0	10

Characterization of NMD -SNVs

Zetasizer was used to measure the PS and PDI of the developed NMD-SNV formulations. The analyses were conducted at 25°C with a scattering angle of 90°. Measurements of the particle mean diameter and PDI were performed after the samples were diluted with distilled water [25,26]. To determine the EE%, the Amicon ultrafiltration method was employed. An ultrafilter was used to spin 4 mL of the NMD-SNV mixture at 3000 rpm for 15 minutes in the top chamber of a centrifuge tube. Using a UV spectrophotometer calibrated to 237 nm, the filtrate's free drug was measured. The EE% was computed using the following formula [27].

$$EE\% = \frac{S-T}{S} \times 100 \quad \text{---------- (1)}$$

T is the actual amount of free drug in each sample, and S is the total amount of drug that is theoretically present in the obtained sample.

Preparation of NTB in situ gel containing NMD

The cold approach was used to create the NMD *in situ* gel. With constant stirring, the cold technique entailed gradually adding varying percentages of poloxamer 407 in cold optimal NMD-SNV together with the preservative (benzylkonium chloride) (Table 2). We kept this dispersion at 4°C for the entire night. The resulting combinations were stored at 4°C for the night [28].

Table 2: Composition of NMD loaded SNV *in situ* gel formulas

Run	NMD (mg/ml)	Poloxamer 407 (%w/v)	NaCl (%w/v)	Benzylkonium Chloride (%w/v)
F1	1	15	0.9	0.01
F2	1	16	0.9	0.01
F3	1	17	0.9	0.01
F4	1	18	0.9	0.01
F5	1	19	0.9	0.01

Characterization of NMD –SNV in situ gel

By adding two milliliters of the chilled formula to a 10-milliliter tube with a 1.0-cm diameter and sealing it with parafilm, the gelation temperature was known. A water bath at a temperature of roughly 4 °C was used to hold the test tube. At the start of the experiment, the water bath temperature gradually rose by 3°C and then by 1°C when it reached the gelation temperature region. The temperature was maintained at this level for 10 minutes after each temperature increased, and the gelation of the solution was monitored. The preparation's meniscus did not shift when the test tube was tilted 90 degrees to verify that gelation had taken place; this was noted as the gelation temperature [29]. The texture analyzer (Stable Micro-Systems, Surrey, UK) was typically used to assess adhesion using probes. Employed the published technique for adhesion measurement, as illustrated in Figure 1 [30,31].

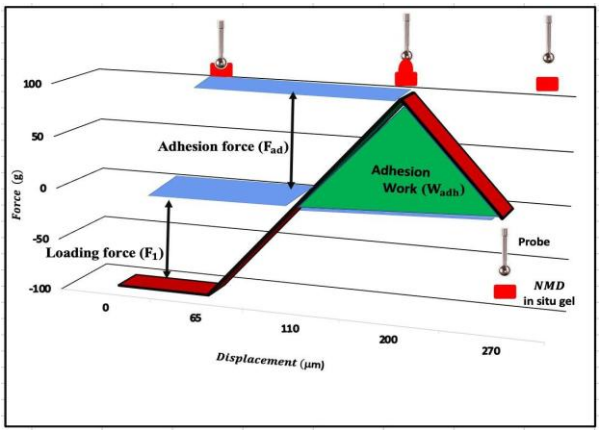

Figure 1: The NMD *in situ* gel is compressed to the value of Fl (loading force), and then the maximum separation force obtained is measured, which is called the adhesion force Fad.

Before reaching a specific loading force (F_1), the spherical indenter gradually moved toward and contacted the *in situ* gel's surface. At one position, where there was no deformation between the gel and the indenter, the force attained equilibrium upon retracting. The break then started at the second point, when the maximum adhesion force was reached. The indent fully separated from the gel at the third position when the relative displacement reached its maximum. The adhesion work required detaching the indenter from the NMD *in situ* gel surface. We pre-equilibrated a 25 g sample of *in situ* gelling formulations in a water bath at 34°C. Slowly, the probe was pushed onto the gel's surface. To guarantee close contact between the probe and the gel's surface, a force of 50 g was applied for ten minutes. It dragged the probe 4 mm away at a rate of 1 mm/s. We measured the force (mN) required to pull the probe away from the gel, which we dubbed the force of adhesion. They calculated the work of adhesion (mN.mm) based on the area under force.

NMD- In situ Gel release study

A five-station dissolution equipment was used for the *in vitro* NMD *in situ* gel release investigation. The USP type I dissolution apparatus (DA8000, Labindia Instruments Pvt. Ltd., Mumbai, India) of the basket type was used in this investigation. For each *in situ* gel, a 3.0 ml formulation containing 1 mg/ml (w/v) NMD was prepared using the technique. As the release medium, 100 ml of stimulated nasal fluid (pH 6.8) (SNF) containing 1% w/v Brgi 35 was used to achieve sink conditions where the solubility of NMD-SNV in SNF equals 3.54. The temperature of the release medium was maintained at 34±0.5°C. The basket's spinning speed was set at 100 rpm. At specified intervals, a new solution of SNF was used in place of the specimen, which had been obtained in a volume of 2.5 ml. A Shimadzu 1900i UV-visible spectrophotometer was used to measure the NMD concentration in the samples at 238 nm. The NMD release research lasted for three hours. Plotting cumulative % NMD release against time in minutes allowed for the calculation of the NMD release kinetics [32,33].

Pharmacokinetic analysis of the optimized NMD loaded SNV

The study used two sets of Wistar albino rats, with six rats each time interval. Rats weighed 250 ± 30 g on average. The rats were put on a heating pad to maintain their body temperatures after receiving an intramuscular injection of ketamine plus zylazine (0.3 ml/250 g rat) to induce anesthesia. For two hours, 0.4 mg/kg animal weight was NMD dosage. To enable the animals in group I to inhale the entire formulation, a micropipette was utilized to gradually infuse a volume of the optimized NMD-SNV (~50 µL) into each nostril over the course of one minute. In contrast, the animals

in group II received an intravenous injection of an NMD vial from the Bayer corporation in their tail vein [34,35]. The University of Baghdad's College of Pharmacy evaluated and approved the study's protocol (RECAUBCP2102023G). After each group received NMD, we took five milliliters of carotid artery blood samples. The animals' brains were then removed from the cranial vault, and the animals were beheaded at intervals of 0.25, 0.5, 0.75, 1, 2, 3, 4, 6, 8, 10, 12, 24, and 48 hours. Separating the plasma from each sample required spinning the blood samples for 10 minutes at 14,000 RPM. We used one milliliter of saline to clean the brain samples. We stored brain tissues and plasma in an ultra-low freezer at -80°C for further pharmacological studies. Two grams of saline were added to each rat brain, and a tissue homogenizer was used to homogenize the tissue at 14,000 RPM. We vortexed 50 µL of cilnidipine internal standard (1000 ng/mL) with either 500 µL of rat plasma or 500 mg of brain sample homogenate for 30 seconds. To extract NMD from brain and plasma samples, three milliliters of tertiary methyl butyl ether were added, and vortexing was done for one minute. The samples underwent a five-minute centrifugation at 3000 RPM and 25°C. A dry, clean tube was carefully filled with two milliliters of the top organic layer of brain and plasma samples. An Eppendorf sample concentrator set to 45°C was used to evaporate the samples. Reconstituting the residue involved a one-milliliter mobile phase. The reconstituted sample was split into two microliters and analyzed using HPLC. They examined brain and plasma samples for NMD using a tried-and-true HPLC technique. They used a Knauer HPLC (Germany) to quantify NMD. Chromatographic separation of NMD and cilnidipine was performed with a Kuanor HPLC-C18 (4.6 x 150 mm, 5 µm) column. At a flow rate of 1.0 mL/min, the isocratic mobile phase—which was composed of acetonitrile and phosphate buffer in a 30:70 ratio—was delivered. The column's temperature stayed at 35°C.

Data analysis

A non-compartmental pharmacokinetic model to determine the drug concentration-time relationship of NMD in brain and plasma tissues. We quickly determined the Cmax and Tmax for intravenous and intranasal delivery based on the concentration-time profile. It was possible to determine the area under the curve AUC0–48 by applying the linear trapezoidal rule to calculate the area under the concentration-time profile. We compared the pharmacokinetic data of groups I and II and examined their statistical significance using Phoenix WinNonlin 6.4 software. We calculated the drug targeting efficiency (%), DTE, and direct transport percentage (%), DTP, for intranasally administered NMD-loaded SNV *in situ* gel based on their AUC values in the brain and plasma. The outcomes were contrasted with those from intravenous injections [34]; equations 2 and 3 were used to calculate these parameters:

$$DTE\% = \frac{(AUCbrain)in/(AUCplasma)In}{(AUCbrain)IV/(AUCplasma)IV} \times 100 \ldots\ldots(2)$$

$$\%DTP = \frac{[\,(AUCplasma)in - Bx.]}{(AUCplasma)in} \times 100 \ldots\ldots\ldots\ldots\ldots(3)$$

Equation 4 determines Bx, or the quantity of NMD that entered the brain through systemic distribution following intranasal administration [36]:

$$Bx = \frac{(AUCplasma)in \times (AUCbrain)IV}{(AUCplasma)IV} \ldots\ldots\ldots\ldots\ldots(4)$$

Where (AUC_{plasma})in, (AUC_{brain})in and (AUC_{plasma})iv, (AUC_{brain})iv stand for the $AUC_{0\text{-}48}$ of NMD in plasma and brain tissues following intranasal and intravenous injection, respectively.

Nasal cilial toxicity study

To assess the nasal toxicity of the improved formulation, histopathological tests were conducted on rats nasal mucosa. *In vivo* administration of three samples into the rats (P1, P2, and P3). As a negative control, P1 was subjected to 100 µL of SNF (pH 6.4); as positive control, P2 received 100 µL of isopropyl alcohol; and P3 was treated for three days with the optimized *in situ* gel formula. Following a three-day period, the rats were decapitated, the nasal was detached, and it was washed with SNF (pH 6.4) and subsequently examined histologically and photographically using a polarizing microscope.

RESULTS

Increasing the Span-60 to Tween-60 ratio from 50:50 in formulas SNV3 and SNV6 to 90:10 and 70:30 in formulas SNV1, SNV4, SNV2, and SNV5, respectively, showed a significant increase in the particle size, polydispersity index, and entrapment efficiency as shown in Table 3.

Table 3: Evaluation parameters of NMD-SNV Formulation

No.	Particle size (nm)	PDI	Entrapment Efficiency (%)
SNV1	143.6	0.1704	87.54
SNV2	73.18	0.1646	81.88
SNV3	43.24	0.159	65.43
SNV4	271.5	0.4865	90.56
SNV5	142.5	0.4721	85.03
SNV6	85.62	0.3608	73.05

The presence of Span 60, Tween 60, and Soluplus influenced particle size, polydispersity index, and entrapment efficiency, which gave different results, as shown by Figure 2A, 2B, and 2C.

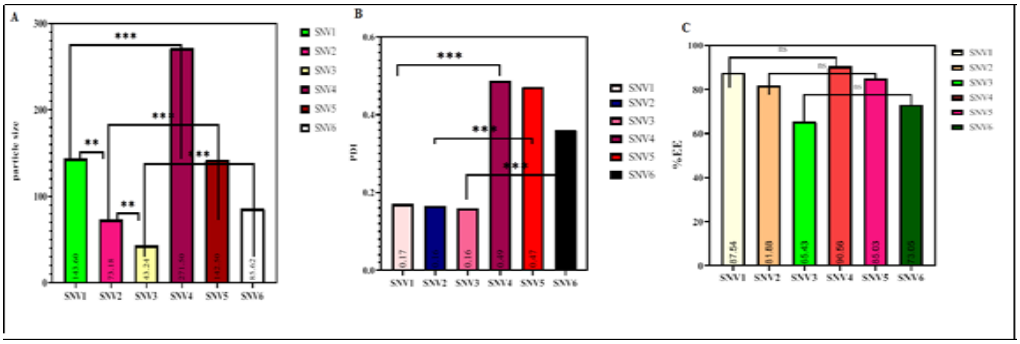

Figure 2: **A**) Effect of span 60 to tween 60 ratio and soluplus on particle size; **B**) Effect of span 60 to tween 60 ratio and soluplus on PDI; **C**) Effect of span 60 to tween 60 ratio and soluplus on % entrapment efficiency.

According to the findings, SNV2 had the greatest desirability score. The calculated SNV2 values for particle size, PDI, and %EE were 73.18 nm, 0.1646, and 81.88%, respectively. Thermo-reversible polymers that are liquid at ambient temperature (20–25°C) and gel at higher temperatures (32–35°C) have been thought to be appropriate for nasal administration of NMD-SNV2. The sol-gel transition temperature of the formulations created is displayed in Table 4. Only one formulation (F3) has a gelation temperature that falls within the permissible range of 32–34°C. All the formulations' drug contents were determined to be within an acceptable range as shown in Table 4.

Table 4: Gelation Temperature and drug content of the NMD-SNV-ISG

Formula	Gelation temperature	Drug content
F1	45	99.8
F2	38	99.9
F3	33	99.9
F4	29	98.9
F5	22	99.1

Loading forces were also calculated from the peak of the force in the negative axis, and adhesion forces were also calculated from the peak of the force in the positive axis. Adhesion work was calculated from the positive area in the force-time plot. Results showed a significant increase in adhesion force and adhesion work as shown in Figure 3.

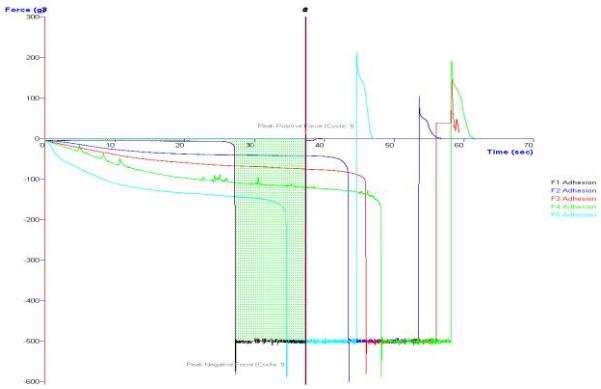

Figure 3: Force–time plot for adhesion work analysis as obtained from TAXTPlus for all *in situ* gel formulation.

Results showed a significant increase in adhesion force and adhesion work as in F2 and F3, which had 106.553±15.3 g, 91.051±9.21 g, and 146.136±18.65 g, 144.403±21.3 g, respectively, compared to F4 and F5, which had 192.985±29.9 g, 238.334±32.2 g, and 215.301±33.5 g, 232.044±37.34 g, respectively, while F1 has a very small amount of adhesion force and adhesion work. Results showed a significant increase in work of adhesion when the % of poloxamer 407 increased from 15 to 19% (w/v), as seen in F1, F2, F3, F4, and F5. The release profiles for NMD from different *in situ* gel formulas were shown in Figure 4.

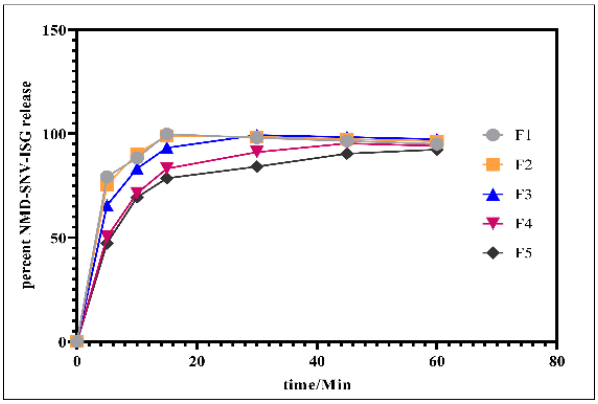

Figure 4: *In vitro* release profile for NMD-SNV-ISG in SNF pH 6.5 at 34±1°C.

The *in situ* gel formula (F1) containing Poloxamer 407 15% w/v showed a higher % release after 15 min equal to 99.8. The *in situ* gel formula F3 containing Poloxamer 407 17% w/v showed a significantly higher % release after 30 min equal to 99.3 than the *in situ* gel formula (F5) containing Poloxamer 407 19% w/v, which showed a low % release after 30 min equal to 84.2. The *in situ* gel formula (F3) was selected as the optimum formula since it showed 99.3% drug release after 30 min, gelation temperature occurred at nasal temperature (33°C), acceptable adhesive force, and good viscosity. The mean plasma and brain drug concentration vs. time curve following intranasal and intravenous administration of NMD nanoformulations is displayed in Figures 5A and 5B, respectively.

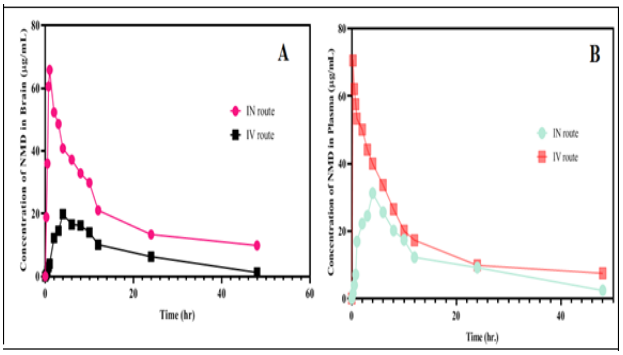

Figure 5: **A**) Concentration–time curve for NMD-SNV *in situ* gel (Intranasal) and NMD-infusion (Intravenous) of brain; **B**) Concentration–time curve for NMD-SNV *in situ* gel (Intranasal) and NMD-infusion (Intravenous) of plasma.

Intranasal delivery of the NMD-loaded SNV2 *in situ* gel intranasal formulation showed a higher brain concentration than intravenous administration of NMD, according to these studies. The pharmacokinetic results in Table 5 indicate that the intranasal NMD-loaded SNV2 *in situ* gel formulation achieved the highest concentration of NMD in the brain and the lowest concentration in plasma, whereas intravenously administered NMD demonstrated the reverse effect. Intranasal delivery of NMD nanoformulations resulted in a significantly higher brain concentration of NMD (p<0.05) than the brain concentrations in animals administered intravenous NMD.

Table 5: Pharmacokinetics Parameters of IN- NMD-SNV and IV-NMD infusion

Formula	Brain			Plasma			Brain targeting parameters	
	C_{max} (µg/ml)	T_{max} (h)	AUC_{0-48} (h.µg/ml)	C_{max} (µg/ml)	T_{max} (h)	AU_{C0-48} (h.µg/ml)	% DTE	% DTP
NMD-SNV IN	65.81	1	938.609	19.88	4	514.108	405.71	54.9
NMD-SNV IV	31.26	4	353.746	70.59	0.25	784.525		

After three days, the nasal ciliotoxicity experiments were conducted to assess the possible harmful effects of excipients included in the formulation on the nasal mucosa. The nasal mucosa treated with PBS (pH 6.4, negative control) exhibited no evidence of inflammation, erosion, or damage to the naso-ciliary region, as shown by Figure 6A, where the nasal membrane remained intact. In contrast, positive control showed significant damage to the nasal mucosa, along with the loss of nasal cilia (Figure 6B). However, with NMD-loaded SNV2 *in situ* gel, damage to the nasal mucosa was not observed, as seen in Figure 6C.

DISCUSSION

One of the most important characteristics of nanocarriers is particle size, which influences cellular absorption, stability, mucoadhesion, drug release profile, biodistribution, and encapsulation efficiency [37]. The results demonstrated that SNV2 and SNV5 prepared using span60 and tween60 at ratio 70:30 had been given the smaller particle size, accepted PDI and efficient entrapment efficiency, which can be explained by the fact that tween 60 have hydrophilic nature and more unsaturation in their chemical structure yield particles of lower size due to their capacity to be compacted easily lead to smaller particle size in SNV2 with acceptance PDI and efficient entrapment efficiency while SNV5 have small particle size but not acceptance PDI and low entrapment efficiency because tween can spontaneously self-assemble into spherical particles, with the majority of the final particles having diameters of less than 50 nm [38–40]. A higher concentration of poloxamer 407 causes micelles to interact more easily, which facilitates the transition to a gel state at a lower temperature. The dense network of micelles forms a structured gel at a reduced gelation temperature.

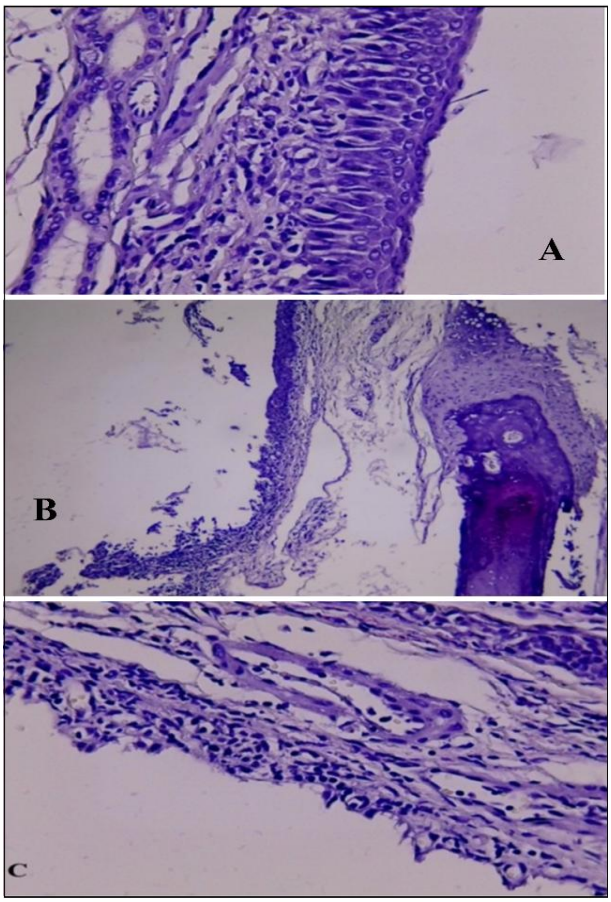

Figure 6: Histopathological examinations of nasal mucosal sections (**A**) Control mucosa, (**B**) IN-SNV *in situ* gel (**C**) positive mucosa.

This lowers the critical micelle temperature (CMT), the temperature at which micelles begin to form, because the high polymer density lowers the energy barrier for micelle formation [41,42]. A denser gel network, higher viscosity, stronger hydrophilic and hydrophobic interactions, and enhanced surface contact area are the reasons for the notable increase in the work of adhesion when the concentration of Poloxamer 407 increases from 15% to 19%. All these elements work together to provide the hydrogel with stronger sticky qualities [43]. High concentrations of poloxamer 407 led to low drug release because the high gel viscosity squeezed inside the aqueous channels by which the drug is distributed between the poloxamer micelles and delayed the drug release [28,44]. According to pharmacokinetic investigations, trigeminal or olfactory pathways may be involved in the direct intranasal distribution of NMD to the brain by intranasal NMD-loaded SNV2 *in situ* gel formulation. On the other hand, DTE was used to evaluate direct medication delivery from the nose to the brain. In this instance, the intranasal NMD-loaded SNV2 *in situ* gel formulation showed the highest values for % DTE, as seen in Table 5. The DTE values fall within the range of 0 and +∞. DTP levels above 0 show that the drug is targeting the brain through the olfactory and/or trigeminal pathways, whereas DTE values above 100 show that the medicine is more effective when administered intranasally as opposed to intravenously [45]. According to the pharmacokinetic analyses conducted on the rats in this investigation, the brain Cmax of intranasal NMD-loaded SNV2 *in situ* gel was approximately 3.3 times greater than that of intravenous NMD. Three rats died in the IV group, whereas there were no deaths in the intranasal delivery of NMD-loaded SNV2 *in situ* gel. A DTP score of 100 means that no medication was absorbed by the body's circulatory system through the indirect route, whereas a high value of % DTE and % DTP obtained with the intranasal NMD loaded SNV2 *in situ* gel formulation indicates that a higher percentage of drug was targeted after intranasal administration while a minimum fraction was taken by the body's circulatory system [46]. These results agreed with that obtained by Gadhave *et al.* and Kumbhar *et al*. [47,48]. According to a nasal ciliary toxicity study, evidence was provided supporting the safety of the excipients included in the formulation. Hence, the constituents of the formulation can be regarded as biocompatible and are unlikely to cause significant histological alterations in the nasal mucosa with prolonged usage [49].

Conclusions

The intranasal NMD-loaded SNV2 *in situ* gel treatment significantly increased the AUC and C_{max} values of the drug in the brains of the animals compared to the intravenous NMD group, according to the investigation of the *in vivo* distribution of NMD in Wistar rats. Applying NMD-loaded SNV2 intranasally improved the permeability of the nasal membrane to NMD, enabling an efficient procedure for NMD brain delivery via the trigeminal or olfactory pathway. A safe and effective formulation for the brain-targeting NMD as a calcium ion channel antagonist for the prevention and treatment of acute subarachnoid hemorrhage can be considered the optimal mucoadhesive NMD-loaded SNV formulation.

ACKNOWLEDGMENTS

The data presented was abstracted from a PhD thesis submitted to the Committee of Graduate Studies, College of Pharmacy, University of Baghdad and the Department of Pharmaceutics. The authors thank the College of Pharmacy, University of Baghdad for providing the resources and instruction necessary to make this work possible.

Conflict of interests

No conflict of interest was declared by the authors.

Funding source

The authors did not receive any source of funds.

Data sharing statement

Supplementary data can be shared with the corresponding author upon reasonable request.

REFERENCES

1. Feigin VL, Rinkel GJ, Lawes CM, Algra A, Bennett DA, van Gijn J, et al. Risk factors for subarachnoid hemorrhage: an updated systematic review of epidemiological studies. *Stroke*. 2005;36(12):2773-2780. doi: 10.1161/01.STR.0000190838.02954.e8.
2. Song X, Jiang Y, Ren C, Sun X, Zhang Q, Gong T, et al. Nimodipine-loaded mixed micelles: formulation, compatibility, pharmacokinetics, and vascular irritability study. *Int J Nanomed*. 2012;7:3689-3699. doi: 10.2147/IJN.S33228.
3. Scriabine A, van den Kerckhoff W. Pharmacology of nimodipine. A review. *Ann N Y Acad Sci*. 1988;522:698-706. doi: 10.1111/j.1749-6632.1988.tb33415.x.
4. Toescu EC, Verkhratsky A. The importance of being subtle: small changes in calcium homeostasis control cognitive decline in normal aging. *Aging Cell*. 2007;6(3):267-273. doi: 10.1111/j.1474-9726.2007.00296.x.
5. Soliman GM, Sharma R, Choi AO, Varshney SK, Winnik FM, Kakkar AK, et al. Tailoring the efficacy of nimodipine drug delivery using nanocarriers based on A2B miktoarm star polymers. *Biomaterials*. 2010;31(32):8382-8392. doi: 10.1016/j.biomaterials.2010.07.039.
6. Langley MS, Sorkin EM. Nimodipine. A review of its pharmacodynamic and pharmacokinetic properties, and therapeutic potential in cerebrovascular disease. *Drugs*. 1989;37(5):669-699. doi: 10.2165/00003495-198937050-00004.
7. Fu Q, Sun J, Zhang D, Li M, Wang Y, Ling G, et al. Nimodipine nanocrystals for oral bioavailability improvement: preparation, characterization and pharmacokinetic studies. *Colloids Surf B Biointerfaces*. 2013;109:161-166. doi: 10.1016/j.colsurfb.2013.01.066.
8. Rashed HM, Shamma RN, Basalious EB. Contribution of both olfactory and systemic pathways for brain targeting of nimodipine-loaded lipo-pluronics micelles: in vitro

characterization and in vivo biodistribution study after intranasal and intravenous delivery. *Drug Deliv*. 2016;24(1):181-187. doi: 10.1080/10717544.2016.1236848.
9. Whii F. Intranasal delivery: Bypassing the blood-brain barrier to deliver therapeutic agents to the brain and spinal cord. *Drug Deliv Technol*. 2002;2(5):46–49.
10. Kapoor M, Cloyd JC, Siegel RA. A review of intranasal formulations for the treatment of seizure emergencies. *J Control Release*. 2016;237:147-159. doi: 10.1016/j.jconrel.2016.07.001.
11. Kumar A, Pandey AN, Jain SK. Nasal-nanotechnology: revolution for efficient therapeutics delivery. *Drug Deliv*. 2016;23(3):681-693. doi: 10.3109/10717544.2014.920431.
12. Zhang QZ, Zha LS, Zhang Y, Jiang WM, Lu W, Shi ZQ, et al. The brain targeting efficiency following nasally applied MPEG-PLA nanoparticles in rats. *J Drug Target*. 2006;14(5):281-290. doi: 10.1080/10611860600721051.
13. Mohsen K, Azzazy HME, Allam NK, Basalious EB. Intranasal lipid nanocapsules for systemic delivery of nimodipine into the brain: In vitro optimization and in vivo pharmacokinetic study. *Mater Sci Eng C Mater Biol Appl*. 2020;116:111236. doi: 10.1016/j.msec.2020.111236.
14. Badria F, Mazyed E. Formulation of nanospanlastics as a promising approach for improving the topical delivery of a natural leukotriene inhibitor (3-Acetyl-11-Keto-β-Boswellic Acid): Statistical optimization, in vitro characterization, and ex vivo permeation study. *Drug Des Dev Ther*. 2020 Sep 15;14:3697-3721. doi: 10.2147/DDDT.S265167.
15. Al-Mahallawi AM, Khowessah OM, Shoukri RA. Enhanced non invasive trans-tympanic delivery of ciprofloxacin through encapsulation into nano-spanlastic vesicles: Fabrication, in-vitro characterization, and comparative ex-vivo permeation studies. *Int J Pharm*. 2017;522(1-2):157-164. doi: 10.1016/j.ijpharm.2017.03.005.
16. Zheng WS, Fang XQ, Wang LL, Zhang YJ. Preparation and quality assessment of itraconazole transfersomes. *Int J Pharm*. 2012;436(1-2):291-298. doi: 10.1016/j.ijpharm.2012.07.003.
17. Pandey M, Choudhury H, Gorain B, Tiong SQ, Wong GYS, Chan KX, et al. Site-specific vesicular drug delivery system for skin cancer: A novel approach for targeting. *Gels*. 2021 Nov 16;7(4):218. doi: 10.3390/gels7040218.
18. Mohammad-Jafari K, Naghib SM, Mozafari MR. Cisplatin-based liposomal nanocarriers for drug delivery in lung cancer therapy: Recent progress and future outlooks. *Curr Pharm Des*. 2024;30(36):2850-2881. doi: 10.2174/0113816128304923240704113319.
19. Mahaki H, Mansourian M, Meshkat Z, Avan A, Shafiee MH, Mahmoudian RA, et al. Nanoparticles containing oxaliplatin and the treatment of colorectal cancer. *Curr Pharm Des*. 2023;29(38):3018-3039. doi: 10.2174/0113816128274742231103063738.
20. Illum L. Blood-brain barrier in drug discovery: Optimizing brain exposure of CNS drugs and minimizing brain side effects for peripheral drugs. John Wiley and Sons; 2015.
21. Wang H, Zhao Y, Wu Y, Hu YL, Nan K, Nie G, et al. Enhanced anti-tumor efficacy by co-delivery of doxorubicin and paclitaxel with amphiphilic methoxy PEG-PLGA copolymer nanoparticles. *Biomaterials*. 2011;32(32):8281-8290. doi: 10.1016/j.biomaterials.2011.07.032.
22. Feng Y, He H, Li F, Lu Y, Qi J, Wu W. An update on the role of nanovehicles in nose-to-brain drug delivery. *Drug Discov Today*. 2018;23(5):1079-1088. doi: 10.1016/j.drudis.2018.01.005.
23. Alhammid SNA, Kassab HJ, Hussein LS, Haiss MA. Spanlastics Nanovesicles: An Emerging and Innovative Approach for Drug Delivery. *Maaen J Med Sci*. 2023;2(2):9. doi: 10.55810/2789-9136.1027.
24. AL-Mansoori MKI, Sabri LA. Preparation and evaluation of transdermal gel loaded with spanlastics containing meloxicam. *J Res Pharm*. 2024;28(4). doi: 10.29228/jrp.801
25. Abdelrahman FE, Elsayed I, Gad MK, Elshafeey AH, Mohamed MI. Response surface optimization, Ex vivo and in vivo investigation of nasal spanlastics for bioavailability enhancement and brain targeting of risperidone. *Int J Pharm*. 2017;530(1-2):1-11. doi: 10.1016/j.ijpharm.2017.07.050.
26. Jaafer H, Al-Kinani KK. Formulation and evaluation of idebenone microemulsion as a potential approach for the transmucosal drug delivery systems. *Iraqi J Pharm Sci*. 2024;33(1):79–88. doi: 10.31351/vol33iss1pp79-88.
27. Rashid AM, Abdal-Hammid SN. Formulation and characterization of itraconazole as nanosuspension dosage form for enhancement of solubility. *Iraqi J Pharm Sci*. 2019;28(2):124–133. doi: 10.31351/vol28iss2pp124-133.
28. Alkufi HK, Kassab HJ. Formulation and evaluation of sustained release sumatriptan mucoadhesive intranasal in-situ gel. *Iraqi J Pharm Sci*. 2019;28(2):95–104. doi: 10.31351/vol28iss2pp95-104.
29. Allah AKA, Abd-Al Hammid SN. Preparation and evaluation of chloramphenicol as thermosensitive ocular in-situ gel. *Iraqi J Pharm Sci*. 2012;21(2):98–105. doi: 10.31351/vol21iss2pp98-105.
30. Gu Z, Wan X, Lou Z, Zhang F, Shi L, Li S, et al. Skin Adhesives with controlled adhesion by polymer chain mobility. *ACS Appl Mater Interfaces*. 2019;11(1):1496-1502. doi: 10.1021/acsami.8b18947.
31. Sun Z, Li Z, Qu K, Zhang Z, Niu Y, Xu W, et al. A review on recent advances in gel adhesion and their potential applications. *J Mol Liq*. 2021;325:115254. doi: 10.1016/j.molliq.2020.115254.
32. Chaturvedi D, Bharti D, Dhal S, Sahu D, Behera H, Sahoo M, et al. Role of stearic acid as the crystal habit modifier in candelilla wax-groundnut oil oleogels. *ChemEngineering*. 2023;7(5):96. doi: 10.3390/chemengineering7050096.
33. Salih OS, Al-Akkam EJ. Preparation, in-vitro, and ex-vivo evaluation of ondansetron loaded invasomes for transdermal delivery. *Iraqi J Pharm Sci*. 2023;32(3):71–84. doi: 10.31351/vol32iss3pp71-84.
34. Abd-Elal RM, Shamma RN, Rashed HM, Bendas ER. Trans-nasal zolmitriptan novasomes: in-vitro preparation, optimization and in-vivo evaluation of brain targeting efficiency. *Drug Deliv*. 2016;23(9):3374-3386. doi: 10.1080/10717544.2016.1183721.
35. Liu S, Yang S, Ho PC. Intranasal administration of carbamazepine-loaded carboxymethyl chitosan nanoparticles for drug delivery to the brain. *Asian J Pharm Sci*. 2018;13(1):72-81. doi: 10.1016/j.ajps.2017.09.001.
36. Alkufi HK, Kassab HJ. Delivery of nose to brain in the management of cerebral vasospasm in aneurysmal subarachnoid hemorrhage. *J Emerg Med Trauma Acute Care*. 2024;2024(6):5. doi: 10.5339/jemtac.2024.absc.5.
37. Azhar Shekoufeh Bahari L, Hamishehkar H. The impact of variables on particle size of solid lipid nanoparticles and nanostructured lipid carriers; A comparative literature review. *Adv Pharm Bull*. 2016;6(2):143-151. doi: 10.15171/apb.2016.021.
38. Alkufi HK, Kassab HJ. Soluplus-stabilized nimodipine-entrapped spanlastic formulations prepared with edge activator (Tween20): Comparative physicochemical evaluation. *Pharm Nanotechnol*. 2024. doi: 10.2174/0122117385348551241028102256.
39. Manar TA, Hanan KJ. Optimizing intranasal amisulpride loaded nanostructured lipid carriers: Formulation, development, and characterization parameters. Vol. 12, Pharmaceutical Nanotechnology. 2024. p. 1–16. doi: 10.2174/0122117385301604240226111533
40. Jaber SH, Rajab NA. Preparation, in-vitro, ex-vivo, and pharmacokinetic study of lasmiditan as iIntranasal nanoemulsion-based in situ gel. *Pharm Nanotechnol*. 2024. doi: 10.2174/0122117385285009231222072303.
41. Kassab HJ, Alkufi HK, Hussein LS. Use of factorial design in formulation and evaluation of intrarectal in situ gel of sumatriptan. *J Adv Pharm Technol Res*. 2023;14(2):119-124. doi: 10.4103/japtr.japtr_603_22.
42. Klouda L, Mikos AG. Thermoresponsive hydrogels in biomedical applications. *Eur J Pharm Biopharm*. 2008;68(1):34–45.

43. Sadeq ZA, Sabri LA, Al-Kinani KK. Natural polymer Effect on gelation and rheology of ketotifen-loaded pH-sensitive in situ ocular gel (Carbapol). *J Adv Pharm Educ Res*. 2022;12(2–2022):45–50. doi: 10.51847/zOf4TcFeKT.
44. Sabri LA, Hussein AA. Comparison between conventional and supersaturable self-nanoemulsion loaded with nebivolol: preparation and in-vitro/ex-vivo evaluation. *Iraqi J Pharm Sci*. 2020;29(1):216–225. doi: 10.31351/vol29iss1pp216-225
45. Lee D, Minko T. Nanotherapeutics for nose-to-brain drug delivery: An approach to bypass the blood brain barrier. *Pharmaceutics*. 2021;13(12):2049. doi: 10.3390/pharmaceutics13122049.
46. Costa CP, Moreira JN, Sousa Lobo JM, Silva AC. Intranasal delivery of nanostructured lipid carriers, solid lipid nanoparticles and nanoemulsions: A current overview of in vivo studies. *Acta Pharm Sin B*. 2021;11(4):925-940. doi: 10.1016/j.apsb.2021.02.012.
47. Gadhave D, Tupe S, Tagalpallewar A, Gorain B, Choudhury H, Kokare C. Nose-to-brain delivery of amisulpride-loaded lipid-based poloxamer-gellan gum nanoemulgel: In vitro and in vivo pharmacological studies. *Int J Pharm*. 2021;607:121050. doi: 10.1016/j.ijpharm.2021.121050.
48. Kumbhar SA, Kokare CR, Shrivastava B, Gorain B, Choudhury H. Preparation, characterization, and optimization of asenapine maleate mucoadhesive nanoemulsion using Box-Behnken design: In vitro and in vivo studies for brain targeting. *Int J Pharm*. 2020;586:119499. doi: 10.1016/j.ijpharm.2020.119499.
49. Barakat NS, Omar SA, Ahmed AA. Carbamazepine uptake into rat brain following intra-olfactory transport. *J Pharm Pharmacol*. 2006;58(1):63-72. doi: 10.1211/jpp.58.1.0008.